Extended Abstracts of the 1994 International Conference on Solid State Devices and Materials, Yokohama, 1994, pp. 461-463

Hot Electron Ballistic Transport in n-AlGaAs/InGaAs/GaAs Small Four-Terminal Structures

Satoshi SASAKI, Yoshiro HIRAYAMA and Seigo TARUCHA

NTT Basic Research Laboratories,
3-1, Morinosato Wakamiya, Atsugi-Shi, Kanagawa 243-01

We have studied hot electron ballistic transport in small four-terminal structures fabricated by Ga focused-ion-beam implantation from an AlGaAs/InGaAs/GaAs modulation doped structure. We have determined the characteristics of negative bend resistance as a function of hot electron energy by analyzing the magneto-resistance data. We have found that the ballistic nature of hot electrons is progressively lost when the excess energy of hot electrons exceeds LO-phonon energy, and that the collimation effect, which is related to the geometry of the electron emitter, is preserved for hot ballistic electrons.

1. Introduction

Recently, transport properties of mesoscopic nanostructures have been extensively studied. Most of the previous investigations were done on the equilibrium transport properties of electrons in AlGaAs/GaAs modulation doped structures which have a very large electron mobility at low temperatures. However, InGaAs-based modulation-doped structures are more suited for the study of the nonequilibrium ballistic transport properties of two-dimensional electrons because the electron mobility is larger compared with that of conventional GaAs-based modulation-doped structures at high temperatures. The high carrier density in this InGaAs-based structures helps not only to increase the mean free path but also to reduce depletion spreading, which is advantageous for fabricating small structures. In such small four-terminal structures formed from AlGaAs/InGaAs/GaAs modulation doped material, ballistic transport has been observed up to room temperature[1]. In this paper, we describe the hot electron ballistic transport characteristics of these structures. We find that the ballistic nature of electron transport is progressively lost when the excess energy of the hot electrons exceeds the LO-phonon energy. We also find that the wave vectors of the ballistic electrons are considerably collimated when the electrons are injected from a narrow terminal and that this collimation appears to be independent of the excess energy of hot electrons.

2. Experimental

Figure 1 shows a plan-view of the four-terminal structure defined by Ga focused-ion-beam (FIB) implantation. The mobility of the AlGaAs/InGaAs/GaAs starting wafer is $6.5\times10^4\,\mathrm{cm^2/V\cdot s}$ below 35 K and decreases down to $7.8\times10^3\,\mathrm{cm^2/V\cdot s}$ as the temperature increases to 290 K. The carrier density is $9\times10^{11}\mathrm{cm^{-2}}$ at low temperatures and $1.1\times10^{12}\mathrm{cm^{-2}}$ near room temperature. Depletion region spreading, including the implanted line width, is about 200 nm. The distance between the facing constrictions, d, over which the injected ballistic electrons travel, ranges from 390 nm to 790 nm. We measure the bend resistance, $R_B = R_{12,43} = V_{43}/I_{12}$, with a high bias voltage, $V_B = V_{12}$, in excess of the LO-phonon energy at temperatures down to 1.5 K. To avoid an increase of the lattice temperature, V_B is applied as square pulses whose width is 20 μs and repetition rate is 100 Hz.

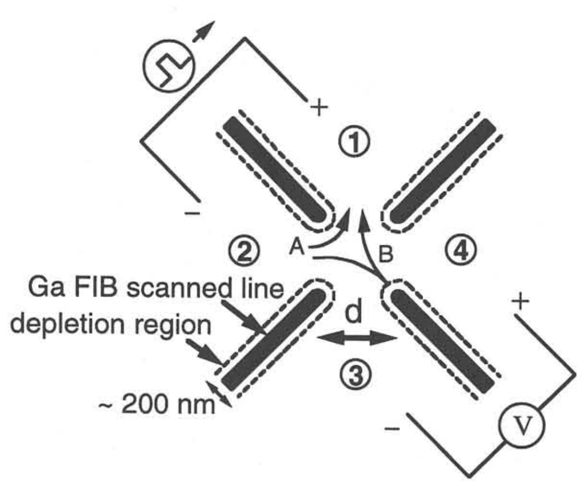

Fig. 1 Schematic plan of a small four-terminal structure fabricated from n-type modulation doped AlGaAs/InGaAs/GaAs material. The configuration for the bend resistance measurement is also shown.

3. Results and Discussion

Figure 2 shows the bend resistance R_B of a sample with d=790 nm observed at T=1.5 K as a function of magnetic field. The second derivative is shown so that the oscillatory component can be more easily seen. The bias voltage V_B increases from 5 mV for the lower most curve to 180 mV for the upper most curve as indicated on the right-hand axis. A distinct negative peak in R_B around B=0 T originates from the ballistic electrons which are incident on voltage terminal 4 after travelling over a distance, d. Shubnikov-de Haas oscillations are observed at high magnetic fields above 1 T. At an intermediate field, B_C, positive peaks are observed in R_B as indicated by the triangles. These peaks are thought to originate from certain electron trajectories such as a focusing trajectory[2] (A in Fig. 1) or a rebouncing trajectory[3] (B in Fig. 1), which are determined by the electron cyclotron motion in the realistic geometry of the lateral constriction in the four terminal structure. We evaluate the critical field B_C which gives rise to the specific electron trajectories by assuming the relation, $B_C = \hbar k_{eff}/eR_C$, where k_{eff} is the effective Fermi wave vector and R_C is the effective cyclotron radius determined from the device geometry.

The peak magnetic field B_C is plotted against the bias voltage V_B in Fig. 3 for several temperatures. B_C increases with increasing V_B at each temperature, which reflects the increase of k_{eff} due to the bias voltage V_B. It should be noted that B_C also increases with temperature at $V_B \approx 0$. This suggests that thermally excited electrons having a wave vector larger than the Fermi wave vector k_F dominate ballistic transport, as previously noted by Hirayama and Tarucha[1].

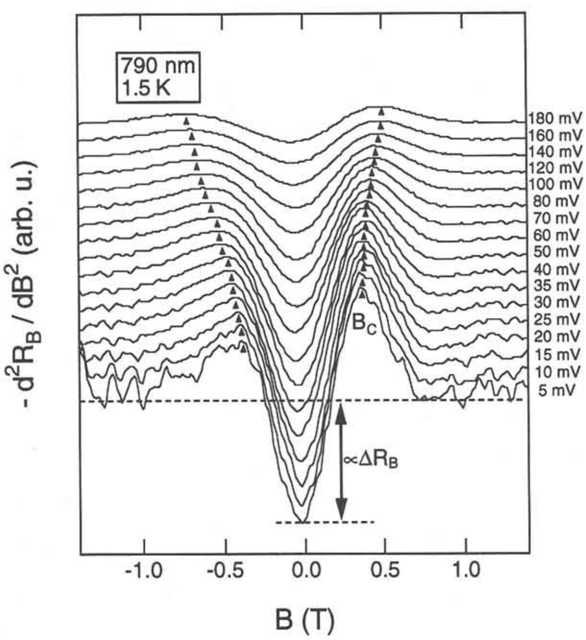

Fig. 2 Second derivative of the observed bend resistance plotted against magnetic field. Triangles (B_C) show the critical magnetic field corresponding to the specific trajectories.

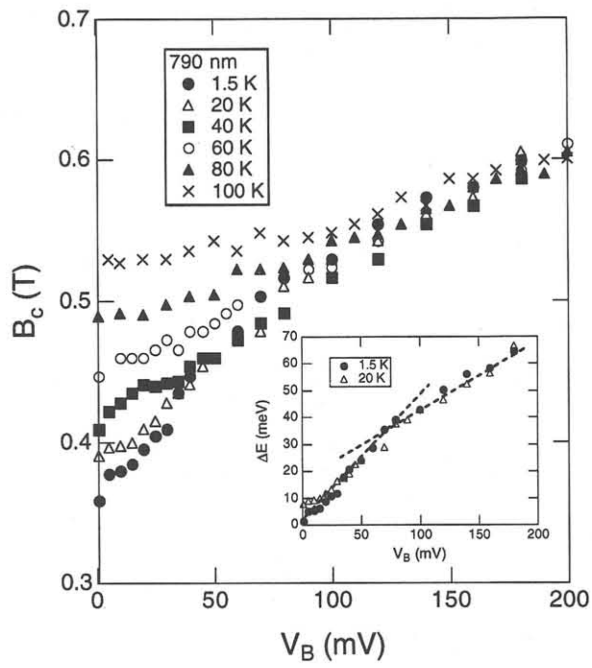

Fig. 3 Focusing magnetic field as a function of bias voltage. The inset shows the excess energy of the injected hot electrons.

The excess energy ΔE of the injected electrons is determined using the relation[4]

$$\frac{B_C(V_B,T)}{B_C(0,0)} = \sqrt{1+\frac{\Delta E}{E_F}}, \qquad (1)$$

where ΔE is measured from the Fermi energy E_F, and is plotted in the inset of Fig. 3 for T=1.5 K and 20 K as a function of V_B. The local voltage drop across the injecting point contact (electron emitter) is nearly half the total applied bias voltage as estimated from the slope of the ΔE against V_B characteristic at low bias region. This slope becomes smaller when ΔE exceeds $\hbar\omega_{LO} \approx 36$ meV, suggesting frequent LO-phonon scattering there. Scattering of electrons into higher lying two-dimensional subbands or the bottom of the GaAs conduction band is negligible because their energies are more than 90 meV above E_F in the present structure.

Figure 4 shows the amplitude ΔR_B of the negative peak around B=0 T as a function of V_B for several temperatures. ΔR_B decreases as the bias voltage or temperature increases probably due to the increase of the acoustic phonon scattering rate for hot electrons. The drop in ΔR_B versus V_B is less prominent for higher temperatures probably because most of the excess energy ΔE for hot ballistic electrons comes from thermal broadening of the electron distribution rather than from the bias voltage[1]. By using the relation of ΔE vs V_B at 1.5 K, we estimate for different temperatures a critical V_B value at which $\Delta E(V_B)$ due to the bias voltage becomes comparable to $\Delta E(V_B$=0) due to the thermal broadening. The estimated V_B values are shown by the arrows in Fig. 4. The drop in ΔR_B becomes larger when V_B is increased beyond these V_B values.

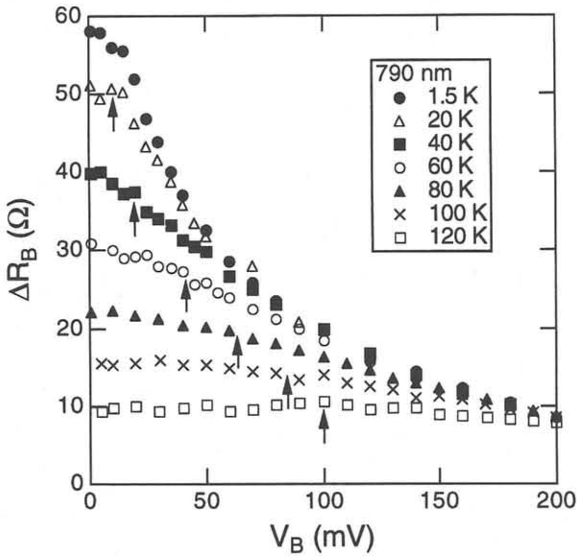

Fig. 4 Bias voltage dependence of the negative peak amplitude. Arrows indicate bias voltages at which the excess energy due to the bias voltage exceeds that due to thermal broadening.

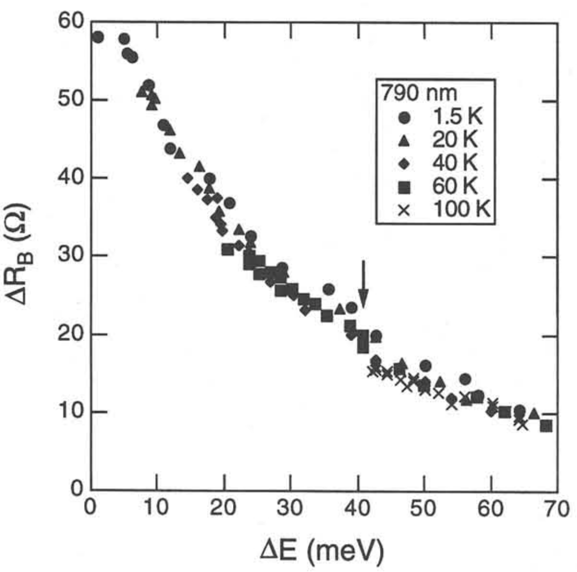

Fig. 5 Negative peak amplitude plotted against excess energy. A kink structure indicated by the arrow appears at around the LO-phonon energy.

In Fig. 5, ΔR_B is plotted against ΔE. Results for different temperatures are almost on the identical curve. This means that ΔR_B is universally described by ΔE regardless of its origin. Moreover, there seems to be a sudden drop in ΔR_B as shown by an arrow around $\Delta E \approx$ 40 meV, in accordance with the kink in ΔE versus V_B plot (see the inset of Fig. 3). We ascribe this structure to the onset of the LO-phonon scattering.

Finally, turning to the collimation effect, Fig. 6 shows the second derivative characteristics of the bend resistance at 1.5 K for a low bias voltage plotted against $d \times B$. The width of the negative peak is compared among samples with different inter-terminal distance d. The inset depicts an electron trajectory at which the negative resistance disappears. The radius of this orbit scales with

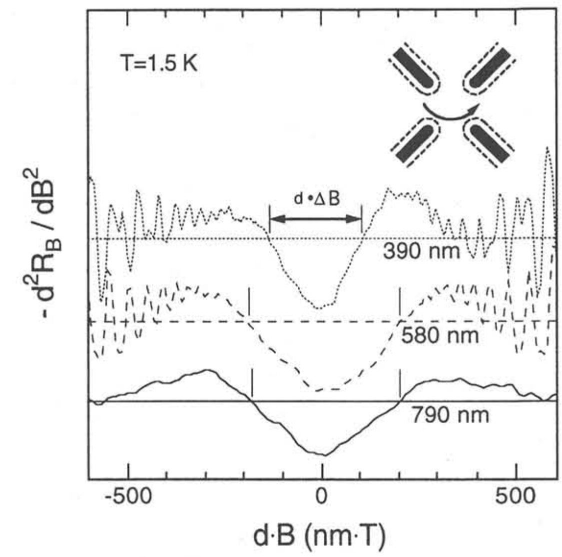

Fig 6 Comparison of the negative peak width among different samples. The inset shows an electron trajectory at which negative resistance disappears.

d. Therefore, the angular distribution of the injected electrons is determined by the value of $d \times \Delta B$, where ΔB is the width of the negative R_B peak[5]. It is clearly seen that this value is considerably smaller in the smallest structure (d=390 nm) than in the larger structures (d >500 nm) because the former has a sufficiently narrow terminal for collimating ballistic electrons. This collimation effect is conserved even for high bias voltages. This indicates that the collimation of the hot ballistic electrons is largely determined by the nature of the injection point contact and that the angular distribution of the electrons does not change even when scattering occurs as long as one only monitors the ballistic electrons.

4. Summary

We have measured the bend resistance of AlGaAs/InGaAs/GaAs small four-terminal structures fabricated by Ga FIB implantation to study the hot electron ballistic transport properties. We have found that the ballistic component of hot electrons rapidly decreases when their excess energy exceeds the LO-phonon energy. We have also found that the wave vectors of the hot ballistic electrons are considerably collimated for samples with a sufficiently narrow injection terminal.

References

1) Y. Hirayama and S. Tarucha: Appl. Phys. Lett. **63** (1993) 2366.
2) Y. Hirayama, S. Tarucha, T. Saku and Y. Horikoshi: Phys. Rev. B **44** (1991) 3440.
3) K. L. Shepard, M. L. Roukes and B. P. van der Gaag: Phys. Rev. B **46** (1992) 9648.
4) J. G. Williamson, H. van Houten, C. W. J. Beenakker, M. E. I. Broekaart and L. I. A. Spendeler: Phys. Rev. B **41** (1990) 1274.
5) L. W. Molenkamp, A. A. M. Staring, C. W. J. Beenakker, R. Eppenga, C. E. Timmering, J. G. Williamson, C. J. P. M. Harmans and C. T. Foxon: Phys. Rev. B **41** (1990) 1274.